doi.org/10.15392/2319-0612.2026.2999
Braz. J. Radiat. Sci., Rio de Janeiro
2026, 14(2) | 01-25| e2999
Editor: Prof. Dr. Bernardo Maranhão Dantas
Editor: Prof. Dr. Alfredo Lopes Ferreira Filho
Submitted: 2025-08-31
Accepted: 2025-12-22

Original Article

Use of geopolymer for cesium sorption

Versieux[a*], J. L.; Freire[a], C.B.; Lameiras[a], F. S.

[a]Center for the Development of Nuclear Technology, 31270-901 - Belo Horizonte – MG - Brazil

*Correspondence: juniara.lversieux@gmail.com

Abstract: The sand extraction plays a crucial role in economic development and the construction industry. However, the fine waste generated during the extraction process brings environmental impacts on this activity. In order to promote the reuse of this waste, the synthesis of geopolymers was proposed. Geopolymers are a class of inorganic materials composed of aluminosilicates arranged in a three-dimensional network, originally developed by Joseph Davidovits in 1978. These are silica–alumina materials with an amorphous to semi-crystalline three-dimensional structure, obtained through alkaline activation. The raw materials used for their synthesis can consist of natural sources of aluminosilicates or by-products from industrial processes, which react through an alkaline activation route, generally using sodium or potassium hydroxide and silicate solutions as activating agents. These materials can be applied in the treatment of liquid radioactive waste through the sorption of cesium, which is commonly present in such waste. The study involved the characterization of mining waste, including quantitative (mineralogical) and qualitative (degree of amorphization) analyses, followed by the synthesis of the geopolymer. After 28 days of curing, the material was ground in a jaw mill and further reduced in a pulverizing mill. Cesium sorption tests with the prepared material were then carried out. The ground geopolymer was characterized by FTIR (Fourier Transform Infrared Spectroscopy), XRD (X-ray Diffraction), XRF (X-ray Fluorescence), particle size analysis, and BET surface area measurement. Cesium sorption tests (using inactive CsCl) were performed using the batch equilibrium method, as described in the EPA Method 530. The results demonstrated that the grinding process was effective in adjusting grain size, enhancing the material's surface area. Mineralogical characterization confirmed the presence of aluminosilicates such as kaolinite and muscovite, which have favorable sorption properties. Thermal analysis identified the temperature range at which the material reaches a stable chemical composition, as well as the regions associated with dehydration and dihydroxylation. The tests indicated that the geopolymer obtained from sand extraction waste showed high cesium sorption potential, as evidenced by the sorption isotherm results.

Keywords: waste, geopolymer, radioactive waste, cesium, sorption.

doi.org/10.15392/2319-0612.2026.2999
Braz. J. Radiat. Sci., Rio de Janeiro
2026, 14(2) | 01-25| e2999
Editor: Prof. Dr. Bernardo Maranhão Dantas
Editor: Prof. Dr. Alfredo Lopes Ferreira Filho
Submitted: 2025-08-31
Accepted: 2025-12-22

Uso de geopolímero para sorção de césio

Resumo: A extração de areia desempenha um papel crucial no desenvolvimento econômico e na construção civil. O resíduo fino gerado durante o processo de extração traz impactos ambientais para esta atividade. Com o objetivo de promover a reutilização desses resíduos, propôs-se sua aplicação na síntese de geopolímeros. Os geopolímeros constituem uma classe de materiais inorgânicos formados por aluminossilicatos dispostos em rede tridimensional, originalmente desenvolvidos por Joseph Davidovits em 1978. Trata-se de materiais sílico-aluminosos com estrutura tridimensional amorfa a semicristalina, obtidos por ativação em meio alcalino. As matérias-primas utilizadas para sua síntese podem consistir em fontes naturais de aluminossilicatos ou em coprodutos oriundos de processos industriais, os quais reagem por meio de uma rota de ativação alcalina, geralmente utilizando soluções de hidróxido e silicato de sódio ou potássio como agentes ativadores. Esses materiais podem ser utilizados no tratamento de rejeitos radioativos líquidos por meio da sorção de césio comumente presente nesses rejeitos. O trabalho consistiu, inicialmente, na caracterização do resíduo de mineração, compreendendo análises quantitativas (mineralógicas) e qualitativas (grau de amorfização); na síntese do geopolímero, seguida de moagem em moinho de mandíbula, posterior redução em moinho pulverizador e, finalmente, na realização do ensaio de sorção de césio com o material obtido. O geopolímero moído, foi caracterizado por FTIR (Espectroscopia no Infravermelho com Transformada de Fourier), DRX (Difração de Raios X), FRX (Fluorescência de Raios X), análise granulométrica com BET. Os ensaios de sorção de césio (utilizando CsCl inativo), foi realizado pelo método de equilíbrio em batelada, conforme descrito na norma EPA 530. Os resultados demonstraram que o processo de moagem foi eficiente na adequação do tamanho de grão, favorecendo o aumento da área superficial do material. A caracterização mineralógica confirmou a presença de aluminossilicatos, como caulinita e muscovita, com propriedades favoráveis à sorção. A análise térmica permitiu identificar a faixa de temperatura em que o material atinge composição química estável, bem como as regiões associadas à desidratação e desidroxilação. Os testes indicaram que o geopolímero obtido a partir do resíduo da extração da areia apresentaram alto potencial de sorção de césio, evidenciado pelos resultados obtidos por meio das isotermas.

Palavras-chave: resíduo, geopolímero, rejeitos radioativos, césio, sorção.

OPEN ACCESS
CC BY

1. INTRODUCTION

Sand extraction plays a fundamental role in the construction industry and in the economic development of the country, providing essential raw material for several industries. However, this activity results in the deposition of waste in dikes and settling ponds, which entails high operational costs, reduces the lifespan of deposits, and causes significant environmental impacts [1]. A viable alternative to mitigate the problems caused by this waste is its use as raw material in the production of new materials, such as geopolymers, thereby contributing to the conservation of natural resources and promoting sustainable initiatives.

Geopolymers are three-dimensional network materials formed from aluminosilicates, similar to natural zeolites, and they were first developed by Joseph Davidovits in 1978. The term "geopolymer" combines the prefix geo, referring to the structural resemblance to naturally occurring minerals, with polymer, which highlights the polymeric arrangement of silica–aluminates [2]. Their polymerization results in the formation of polysialates, an abbreviated designation for silicon-oxo-aluminates (Si–O–Al). Polysialates consist of Si^{4+} and Al^{3+} units in tetrahedral coordination with oxygen atoms, linked through covalent and ionic bonds, forming rings and chains with high structural stability [3]. The geopolymerization process requires the presence of charge-balancing cations to compensate for the isomorphic substitution of Si^{4+} by Al^{3+} in the network, which are often supplied by raw materials such as kaolinite or metakaolinite [4]. These materials offer several advantages, including high thermal and mechanical resistance, as well as the ability to replace conventional products such as cements, plastics, and industrial minerals [3].

According to the literature, several studies demonstrate that geopolymers are highly effective materials for the containment of toxic waste due to their ability to immobilize heavy metals and radioactive elements [5] and [6]. This performance is related to the tridimensional aluminosilicate framework of these materials, whose formation and activation mechanisms

OPEN ACCESS

are widely discussed in the foundational works by Provis and collaborators on alkali-activated binders [7] and [8].

The growing interest in alkali-activated materials, such as geopolymers, is driven by the increase in population and, consequently, the generation of waste and the demand for alternative raw materials [1]. Geopolymer synthesis generally involves raw materials rich in silica and alumina, such as kaolinite ($Al_2Si_2O_5(OH)_4$). After calcination, this clay loses most of its hydroxyl groups (OH^-), becoming an amorphous and highly reactive aluminosilicate [4].

Another important aspect highlighted in this study concerns radiation sources. They have numerous beneficial applications for society, including electricity generation, medical use, food processing, environmental monitoring, and agriculture. However, these applications also generate radioactive waste that requires appropriate treatment and storage. Among the various approaches employed for the treatment of such waste, coagulation, ion exchange, membrane filtration, and sorption stand out [9]. Sorption, in particular, has gained prominence in the scientific literature due to its low cost, operational simplicity, and high efficiency [10]. The results were evaluated through statistical analysis and sorption isotherms.

2. MATERIALS AND METHODS

Initially, the characterization of the sand-extraction residue was carried out for both qualitative and quantitative analyses, in order to verify whether the material exhibited physicochemical properties suitable for subsequent applications. The analyses aimed to determine the mineralogical composition, particle-size distribution, surface area, and thermal behavior of the residue. For this purpose, the following techniques were employed: FTIR (Fourier Transform Infrared Spectroscopy), XRD (X-ray Diffraction), XRF (X-ray Fluorescence), particle size analysis, and BET surface area measurement.

Particle-size distribution was determined by laser diffraction using a Cilas 1190 Liquid analyzer, from the Nanotechnology Service (SENAN/CDTN), located at the Nuclear Fuel

OPEN ACCESS
cc BY

Laboratory (LABCOM/CDTN). Moisture content was evaluated according to Technical Routine 417 of the Cementation Laboratory (LABCIM/CDTN, 2005), which consists of drying the sample at 105 ± 5 °C until constant mass is achieved. The difference between wet and dry mass was expressed as the moisture content, in percentage.

After characterization, the residue was calcined at 800 °C for 4 hours, with a heating rate of 10 °C/min. The calcined material was then homogenized with the activating solution, composed of sodium silicate and a 10 M sodium hydroxide solution, in an electromechanical 5-L concrete mixer (Figures 1a and 1b). The mixture was prepared using 65% residue, 20% sodium silicate, and 15% sodium hydroxide, proportions defined based on the authors' previous studies on geopolymers produced from calcined waste. This procedure followed Brazilian Standards ABNT NBR NM 52 [11] (Determination of Consistency of Hydraulic Cement Mortar) and ABNT NBR 7215 [12] (Determination of the Compressive Strength of Hydraulic Cement Mortars).

The mixture was placed into cylindrical PVC molds, 5 cm in diameter and 10 cm in height, and subsequently subjected to vibration for 60 seconds in a Bruni alti linear pneumatic vibrator, model NTS (Figures 1c and 1d). According to the literature [13], both the compaction process and vibration influence the water absorption capacity of geopolymer monoliths.

Figure 1: (a) Electromechanical mortar mixer; (b) Mixing of the calcined residue with the activating solution; (c) Molding of cylindrical specimens; (d) Vibration of cylindrical specimens

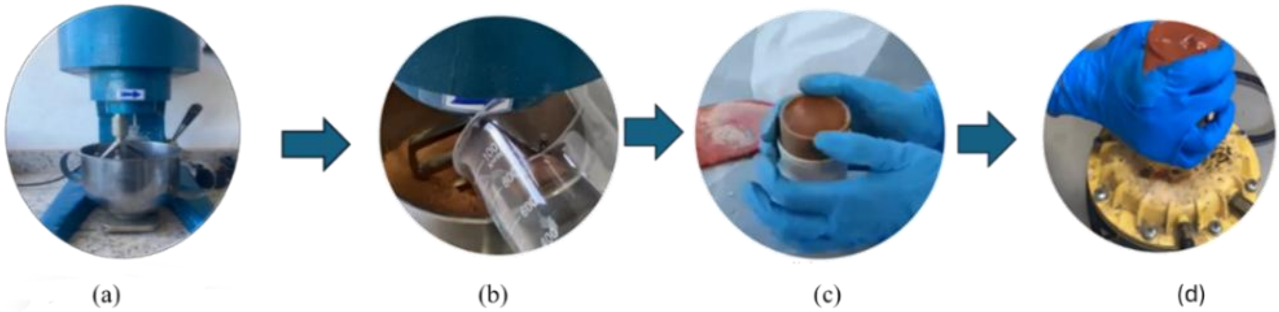

Source: Author (2024).

After 24 hours, the cylindrical specimens were demolded and cured at room temperature for 28 days (Figures 2a and 2b). Subsequently, the material was ground using a drum-type pulverizing mill manufactured by AMEF. Figure 2c illustrates the appearance of the geopolymer after the grinding process that be used as sorbent material in the batch equilibrium test.

Figure 2: (a) Cylindrical specimens being demolded; (b) Cylindrical specimens under ambient curing; (c) Geopolymer aspect after the grinding process

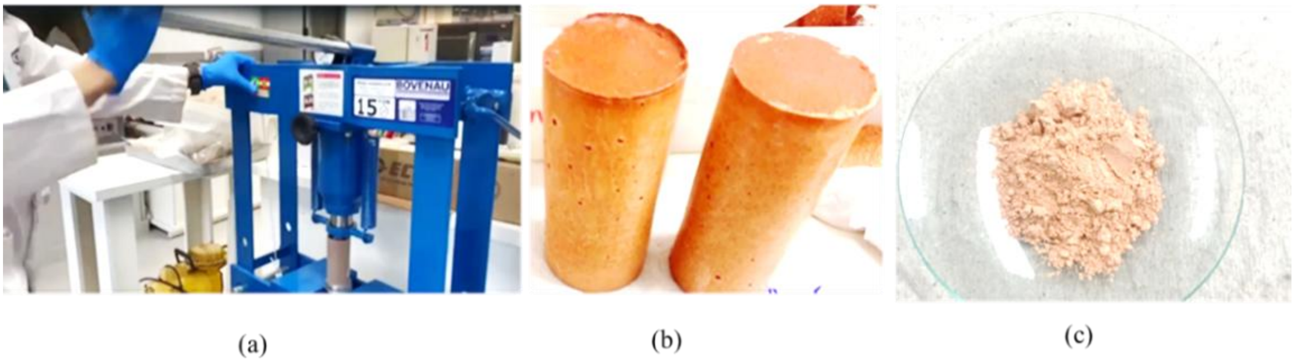

Source: Author (2024).

Cesium sorption tests were subsequently carried out using the batch equilibrium method, aiming to evaluate the sorption capacity of the ground geopolymer. The batch equilibrium test consists of placing the sorbent material, in this case, the ground geopolymer, in contact with an aqueous solution containing CsCl at concentrations determined for each stage.

The tests followed the procedures established in EPA Method 530 [14], which are divided into three stages: determination of the geopolymer: CsCl solution ratio most favorable for sorption (stage 1); determination of the equilibrium time (stage 2) and construction of the sorption isotherm (stage3). For all stages, agitation was performed using a rotary shaker (Figure 3), designed in accordance with the specifications of EPA Method 530 [14] and available at the facilities of LABCIM/CDTN.

OPEN ACCESS
cc BY

Figure 3: Rotary shaker according to the specifications of EPA Method 530

Source: Author (2024).

The geopolymer-to-solution ratios used in stage 1 are presented in Table 1, along with the corresponding masses of ground geopolymer employed as the sorbent material in 200 mL of CsCl solution, prepared at a concentration of 0.43 g.L^{-1}. The cesium chloride concentration was defined based on the value of 340 mg.L^{-1} of Cs^{+} established in the study by Freire [15], which investigated the sorption of cesium and strontium in Brazilian clays for potential use as barriers in radioactive waste repositories. The proportions adopted in this study are consistent with EPA Method 530, which recommends solid-to-liquid ratios ranging from 1:4 to 1:500.

Table 1: Geopolymer: solution ratios for ground geopolymer used as sorbent material

BOTTLES IDENTIFICATION	GEOPOLYMER: SOLUTION RATIO (g: mL)	ACTUAL MASS OF GEOPOLYMER (M_R) (g)	MASS OF GEOPOLYMER USED (M_U) (g)
1GA1	1:4	50.00	53.58
1GA2	1:10	20.00	21.43
1GA3	1:20	10.00	10.72
1GA4	1:40	5.00	5.36
1GA5	1:60	3.30	3.54
1GA6	1:100	2.00	2.14
1GA7	1:200	1.00	1.07
1GA8	1:500	0.40	0.43

*1GA1 - stage 1; G - Ground geopolymer; A - Sample; 1 - Ratio 1; *Mr - actual mass considering moisture; *Mu- actual mass disregarding moisture.

Source: Authors (2024).

For each ratio, a blank was prepared containing only the cesium chloride solution (340 mg.L^{-1}), without contact with the sorbent. The blank was agitated and filtered under the same conditions as the tests performed with the samples. The systems were kept under constant agitation (29 ± 2 rpm) for 24 ± 0.5 h at 25 ± 3 °C. Solid–liquid separation was carried out by vacuum filtration using a membrane (0.45 μm), as shown in Figure 4.

Figure 4: Filtrate collected for XRF analysis (Thermo QUANT'X spectrometer) to quantify cesium

Source: Authors (2024).

The adsorbed percentage (%A), representing the sorption capacity, was calculated using equations described in the referenced method [14]. Concentrations in the initial solution and in the filtrate were used for the calculations for each proportion. The proportion that resulted in a %A value between 10% and 30% was selected for stage 2

In stage 2, the ideal equilibrium time was determined. The ratio selected in the previous stage was subjected to agitation periods of 1, 24, 48, and 72 hours. Agitation (29 ± 2 rpm) and ambient temperature were monitored throughout. After each interval, the samples were filtered. Cs^+ concentrations were determined by XRF. For each time interval, the change in solute concentration, in this case, CsCl, before and after agitation was calculated using the equation described in the referenced method [14].

For stage 3, the agitation time was set to the interval during which the solute concentration variation was equal to or less than 5% over 24 hours, indicating that the concentration had essentially stabilized. According to EPA Method 530 [14], eight dilutions were prepared (Table 2) to construct the adsorption curve.

Table 2: Cesium chloride solution concentrations for stage 3 using ground geopolymer

SAMPLE CODE*	DILUTION NUMBER	CSCL SOLUTION CONCENTRATION (MG. L-¹)
3AD1G	1	340
3AD2G	2	170
3AD3G	3	110
3AD4G	4	80
3AD5G	5	70
3AD6G	6	40
3AD7G	7	20
3AD8G	8	10

*3AD1C: stage 3, sample, dilution 1, ground geopolymer

Source: Authors (2024).

At the end of stage 3, filtration was carried out, as in the previous stages, and the samples were sent for determination of cesium (Cs^+) concentration using XRF.

Based on the results obtained the Cs^+ concentration in the stock solution (C_0), in the samples (C), and in the blank (C_B), the sorption isotherm (x/m versus C) was plotted.

3. RESULTS AND DISCUSSIONS

3.1. Results of the sand-extraction residue

Based on the results of X-ray fluorescence (XRF) analysis for the calcined residue, presented in Table 3, the molar ratio of SiO_2/Al_2O_3 was calculated, yielding a value of 3.04:1. This value indicates that the residue has a moderately adequate proportion of silica and alumina for geopolymerization reactions. According to the literature [3], the best performance in geopolymer formation is observed when this ratio ranges from 3.3:1 to 4.5:1. Values below this range may result in less dense structures, whereas excessive values can hinder the formation of the polymeric gel [13]. The sum of SiO_2, Al_2O_3, and Fe_2O_3 totaled 83.88%, classifying the material as of medium reactivity, according to [4].

Table 3: XRF results for clay (CDTN, 2023)

COMPONENT	MASS (%)
SiO_2	53.28
Al_2O_3	28.92
CaO	0.08
MgO	0.80
Fe_2O_3	1.68
Molar ratio SiO_2/Al_2O_3	3.04: 1
$SiO_2 + Al_2O_3 + Fe_2O_3$	83.88

Source: Authors (2024).

Fourier-transform infrared spectroscopy (FTIR, Figure 5) revealed characteristic bands of aluminosilicate materials, confirming that the residue is composed of phases derived from clay minerals. The broad band between 3200 and 3700 cm^{-1} is attributed to O–H stretching vibrations associated with the structural hydroxyl groups of kaolinite [13]. In the region between 1200 and 200 cm^{-1}, absorptions consistent with Si–O–Si and Si–O–Al vibrations were observed, indicating the presence of muscovite, a mica-type phyllosilicate with an approximate composition of $KAl_2(Si_3AlO_{10})(OH)_2$ [16]. The coexistence of kaolinite and muscovite aligns with the typical mineralogical profile of industrial clay-based residues.

Figure 5: Infrared spectroscopy of mining waste

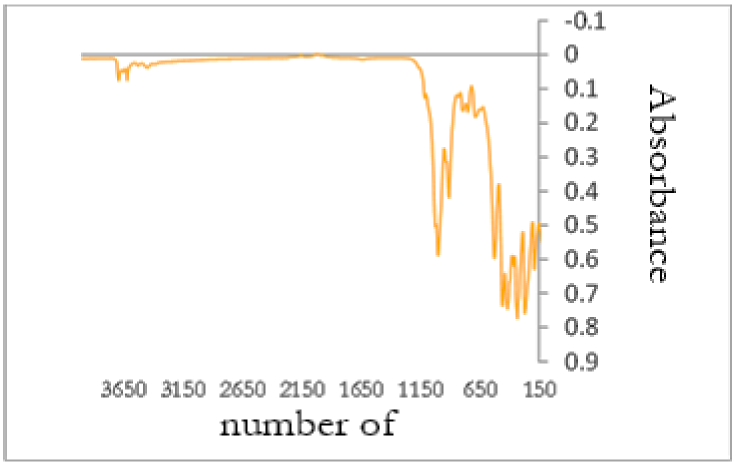

Source: Author (2024).

OPEN ACCESS

Particle size analysis (Figure 6) revealed that the residue has an average particle diameter of 16.79 µm, consistent with the typical range observed for clay minerals [17].

Characterization by the BET method (Brunauer–Emmett–Teller) indicated a specific surface area of 11.66 $m^2 \cdot g^{-1}$, while the total surface area was 24.26 m^2, suggesting that the material exhibits a particulate and potentially porous matrix. The specific surface area corresponds to the total area available per unit mass and is particularly sensitive to particle size and solid porosity; the total surface area, in turn, represents the sum of all external and internal surfaces accessible for adsorption, regardless of the mass involved. High values for these parameters are typical of reactive materials with substantial surface exposure, conditions that enhance the dissolution of precursor phases and increase the number of reactive sites during geopolymerization [18].

Figure 6: Particle size analysis of the mining residue

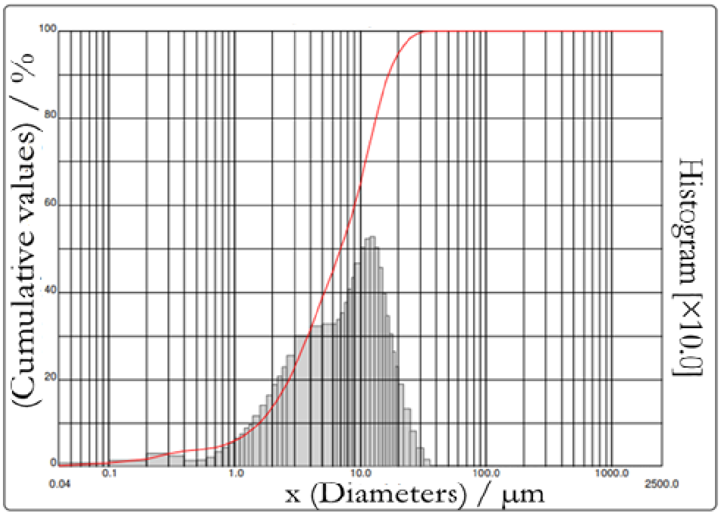

Source: Authors (2024).

Thermal analysis of the residue (Figure 7) enabled the identification of the main physicochemical transformations occurring as a function of temperature.

The first endothermic event, observed at 79.3 °C, is associated with the removal of physically adsorbed water, resulting in a mass loss of approximately 1.44%. This is followed by another endothermic event at 261.0 °C (−0.22%/min), corresponding to the elimination of crystallization water and the decomposition of residual organic matter present in the raw residue.

Between 400 and 650 °C, the characteristic dehydroxylation of kaolinite can be observed, evidenced by a pronounced endothermic peak at 532.6 °C (−0.59%/min), with an onset at 489.9 °C. This stage leads to the formation of metakaolinite, an amorphous and highly reactive phase that plays a fundamental role as a precursor in geopolymer synthesis.

Starting at 800 °C, a slight additional mass loss is observed, totaling about 8.26%, which is attributed to the partial decomposition of muscovite. This behavior aligns with the typical thermal degradation of aluminosilicate micas and reinforces the presence of this mineral, previously identified through spectroscopic and mineralogical analyses [19] and [20].

Finally, a pronounced exothermic peak at 940.9 °C marks the crystallization of mullite, a stable phase derived from the thermal transformation of metakaolinite.

Together, the thermal analysis results demonstrate that the residue exhibits a sequence of transformations typical of aluminosilicate materials containing kaolinite and muscovite. The selection of 800 °C as the ideal calcination temperature was based on the references cited in this study, previous investigations reported in the literature, and additional work carried out at CDTN by different researchers in the group.

Figure 7: Thermal analysis of clay

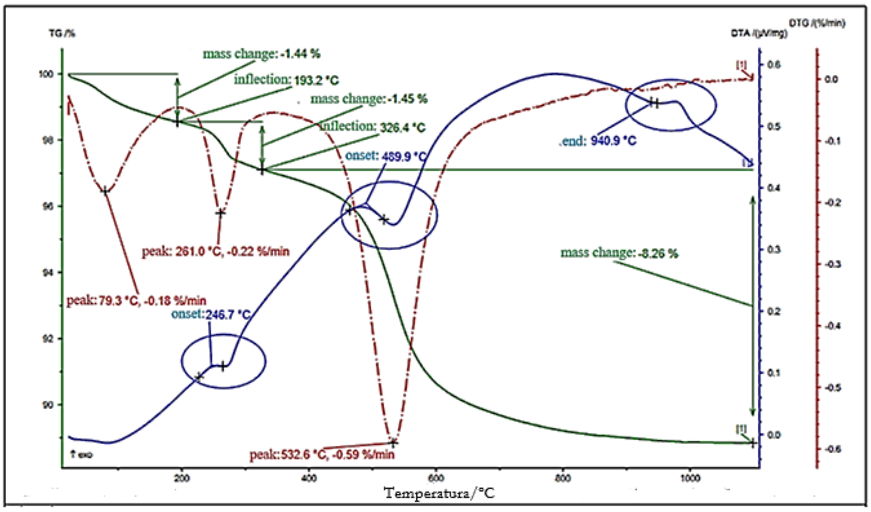

Source: CDTN (2024).

The X-ray diffraction (XRD) analysis of the residue (Figure 8) revealed a crystallographic pattern characteristic of clay-based materials composed of aluminosilicate phases. The diffractogram exhibits well-defined peaks confirming the predominant presence of kaolinite and muscovite, minerals typically found in sedimentary clay materials and commonly associated with industrial silicate-based residues.

Kaolinite was identified through its characteristic reflections located at approximately 12.3°, 20.4°, 24.9°, 35°, and 38° (2θ) [21]. These peaks indicate a relatively well-preserved crystalline structure, typical of materials that have not undergone prior calcination. Muscovite, a mica-type phyllosilicate, was recognized by the intense peaks near 8.8°, 17.8°, 26.6°, 45°, and 50° (2θ), corresponding to the basal and prismatic planes of the mineral [21].

In addition to the main aluminosilicate phases, minor mineral components were also identified. Weak reflections near 21°, 33°, and 36° (2θ) indicate the presence of goethite (α-FeO(OH)) [21], suggesting small amounts of iron oxides/hydroxides associated with the original material. Quartz (SiO_2) was also detected, evidenced by the sharp peaks at approximately 20.8°, 26.6°, and 50° (2θ), characteristic of its trigonal lattice.

Figure 8: X-ray diffraction of the clay residue

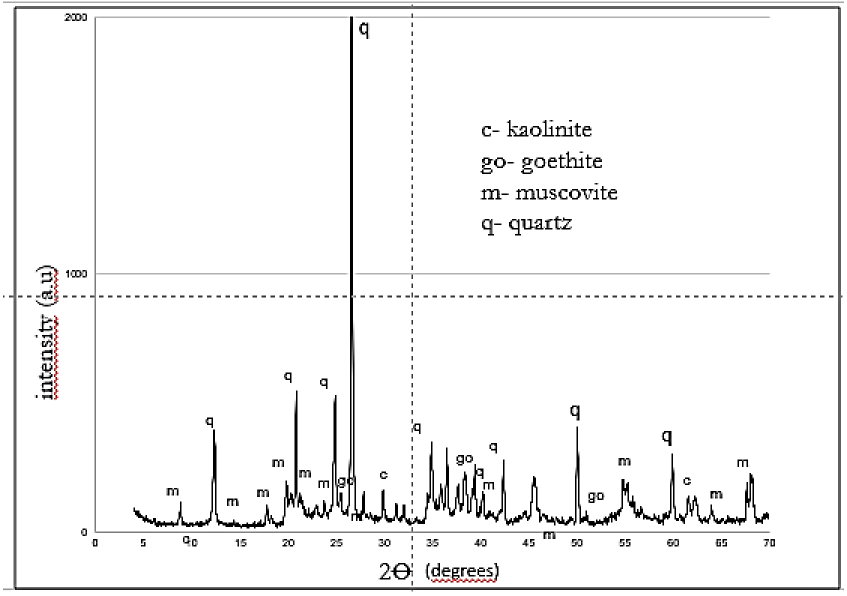

Source: Geotechnology Solutions Company (SOLOCAP) (2024).

3.2. Characterization of the Geopolymer after Grinding

According to the BET analysis (Figure 9), the material exhibited an average particle diameter of approximately 32 µm and a total surface area of 11.81 $m^2.g^{-1}$. Although this surface area is relatively low compared to highly porous adsorbents, recent studies have shown that moderate specific surface areas do not prevent geopolymers from achieving satisfactory performance in sorption processes. Recent work has demonstrated that geopolymers with specific surface areas around 82 $m^2.g^{-1}$ were able to efficiently remove pharmaceutical contaminants, emphasizing that characteristics such as pore-size distribution and surface chemical properties strongly influence adsorptive behavior [22]. Similarly, Genua et al. [23] highlight that, although larger surface areas increase the number of available sorption sites, factors such as porosity, internal connectivity, and the structure of the geopolymeric matrix also play a significant role. Therefore, the decision to work with a particle size of approximately 32 µm was made with the aim of reducing the energy consumption associated with the grinding process, considering that the literature indicates that sorption efficiency depends on multiple factors beyond specific surface area.

Figure 9: Particle size distribution of the ground geopolymer

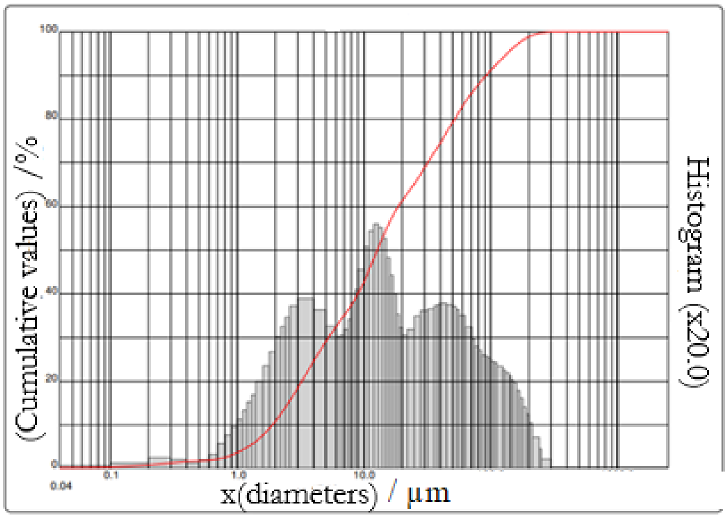

Source: Authors (2024).

OPEN ACCESS

The thermal analysis of the geopolymer (Figure 10) reveals a well-defined endothermic event below 200 °C, observed simultaneously in the DTA (red) and DTG (blue) curves. In the DTA curve, this behavior appears as an endothermic deviation indicating heat absorption, while the DTG curve displays a peak corresponding to the highest rate of mass loss within the same temperature range. The TG curve (green) shows a mass loss of approximately 13–14%, with the first onset point occurring at around 81 °C, coinciding with the main low-temperature endothermic event.

This behavior is consistent with the material's processing history. Because the geopolymer was produced from a previously calcined residue, most of the water had already been removed during calcination. Additionally, during geopolymerization, water acts merely as a reaction medium and is not permanently incorporated into the aluminosilicate gel structure [24].

This result aligns fully with the other characterizations and with the low moisture content observed in the batch equilibrium experiments (mean value of 7.03%), reinforcing that the material exhibits low water retention.

Figure 10: Thermal analysis of the geopolymer after grinding

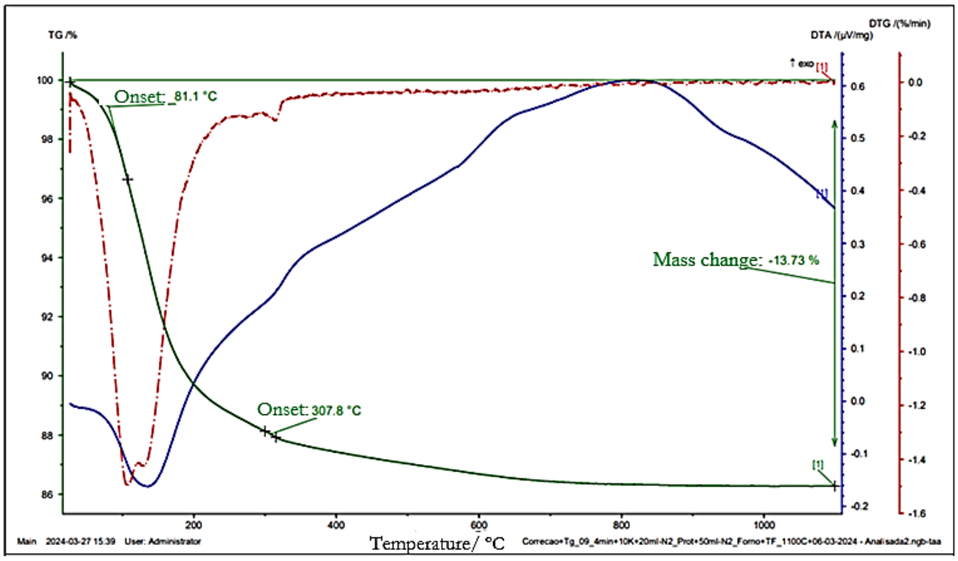

Source: Author (2024).

OPEN ACCESS

3.3. Results of the Cesium Sorption Stages with the Geopolymer

The results from the determination of the geopolymer: solution ratio (stage 1) are presented in Table 4. These results allowed evaluation of the material's performance, with sorption capacities exceeding 50% for all ratios tested and reaching values close to 98% for some ratios. To ensure the reliability of the results, the samples were also analyzed by XRF (energy-dispersive). Both techniques yielded consistent results with minimal discrepancy between them, reinforcing the robustness of the data obtained.

Table 4: Results of stage 1 of the sorption test for the geopolymer

SAMPLE CODE	SOLUTE: SOLUTION RATIO (g:mL)	CS$^+$ CONCENTRATION (mg. L^{-1})	SORPTION CAPACITY (%A) – XRF ANALYSIS
1GA1	1:04	241	97.71
1GA2	1:10	284	97.28
1GA3	1:20	355	97.11
1GA4	1:40	287	96.76
1GA5	1:60	345	93.67
1GA6	1:100	286	85.48
1GA7	1:200	351	82.65
1GA8	1:500	313	59.64

Source: Authors (2024).

In stage 2, the 1:500 ratio was used, corresponding to 0.43 g of geopolymer in 200 mL of CsCl solution, as defined in stage 1. According to the method, the ideal ratio is that for which the absorption percentage (%A) falls between 10% and 30%. Experimental conditions were kept constant: agitation at 29 ± 2 rpm, temperature of 25 ± 3 °C, and pH close to 7.5. Aliquots were analyzed by X-ray fluorescence (XRF).

Based on the results obtained from the analysis of the filtrate, a curve for this stage was constructed, relating the equilibrium cesium concentration to contact time (Figure 11). The percentage change in concentration (%ΔC) between the initial solute concentration (C_1) and the concentration after the agitation period (C_2) was also calculated. The observed variations for the intervals 1–24 h, 24–48 h, and 48–72 h were 38%, 3%, and -10%, respectively.

The negative value observed for the concentration variation between 48 and 72 h can be explained by the occurrence of desorption processes, since sorption is not necessarily permanent and desorption is a natural component of equilibrium in aqueous systems [25].

During the sorption experiment, it was recorded that, after the 48 h, rotation time, a change in the suspension's pH occurred (from approximately 5 to around 6), which altered the chemical conditions of the medium and consequently promoted slight solute desorption. According to the literature [26], in many systems adsorption is a reversible process, and desorption occurs when there are changes in chemical conditions (such as pH, ionic strength, or ionic competition) or when the system reaches equilibrium from the opposite direction.

Consistent with this behavior, another study demonstrated that even after the equilibrium time is reached, desorption may remain measurable and exert a significant influence on the mobility of metals and radionuclides in solid systems [27].

Furthermore, the adsorbent material used in this research is not a natural clay, but rather a geopolymer, whose surface may contain amorphous aluminates and silicates.

These results confirmed the good performance already observed in stage 1.

The concentration versus time curve indicated that the highest sorption values occur within the first hours, reaching approximately 50% in less than 24 h. Therefore, the equilibrium time adopted was 24 h, in accordance with EPA 530 [14], as the concentration variation during this interval was below 5%.

It was observed that the adsorption kinetics exhibited two distinct phases: an initial rapid phase attributed to surface sorption, followed by a slower phase associated with intraparticle diffusion.

OPEN ACCESS

Figure 11: Cs$^+$ Concentration as a function of time - sorption with geopolymer after grinding

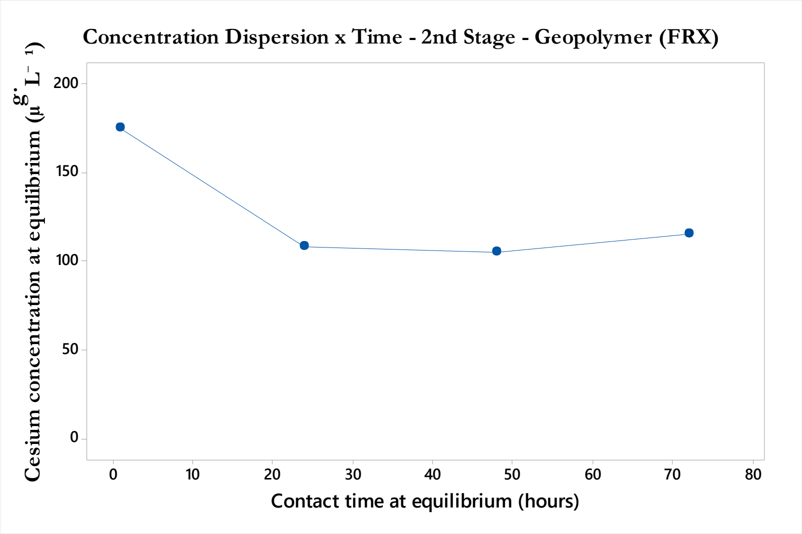

Source: Authors (2024).

In stage 3, the adsorption capacity of the geopolymer after grinding was determined based on the cesium concentration in the filtrate (C) and the amount of cesium adsorbed per unit mass of the material (x/m). From these data, the sorption isotherm was constructed (Figure 12). The adsorption behavior observed, particularly at high Cs$^+$ ion concentrations, may be related to the limited availability of adsorption sites. As the ion concentration in the solution increases, these sites become progressively less available. This capacity, however, can be enhanced by increasing the specific surface area of the adsorbent material. In materials with high surface area, even small quantities can contain a large number of available sorption sites.

The linear fit of the experimental results indicates that the isotherm behavior follows the classical Langmuir model, revealing typical homogeneous surface behavior and monolayer formation. According to Santos [28], this type of linear behavior is commonly observed when the number of adsorption sites available exceeds the solute concentration in the solution.

Figure 12: Langmuir model for cesium sorption with geopolymer

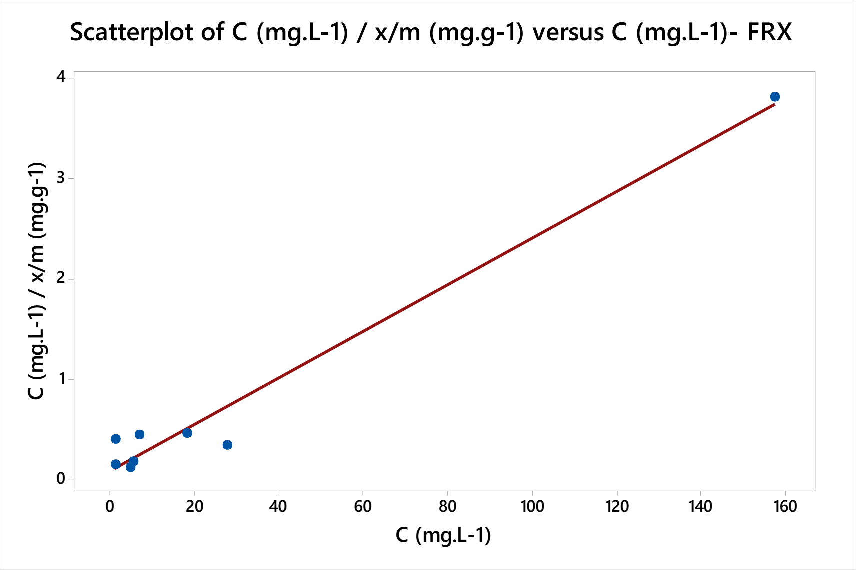

Source: Authors (2024).

The Langmuir parameters and the results of the linear regression are presented in Tables 5 and 6. The linear regression coefficient (R^2) indicated that, after a series of experimental measurements, the Langmuir model provides a good representation of the sorption data. Additionally, the p-value was below the significance level, and the calculated F-value was significantly higher than the critical F (F of significance), indicating that the analysis was statistically significant.

The parameter M represents the concentration of solute adsorbed, corresponding to the maximum monolayer adsorption capacity. The parameter K_L expresses the affinity of the adsorbate, i.e., Cs^+, for the adsorbent surface, which in this analysis is the geopolymer. The results obtained for the K_L and M parameters demonstrate the high performance of the material as an adsorbent. The significant value of M indicates a remarkable capacity for solute retention on the geopolymer surface. Similarly, the K_L parameter, which reflects the affinity between the adsorbate and adsorbent, showed values that reveal a strong interaction between the cesium ion and the geopolymer adsorbent material.

OPEN ACCESS
cc BY

Table 5: Langmuir model parameters for geopolymers

K_L (L.g-1)	M (mg. g-1)	R^2 (%)	R^2 (pred) (%)
55.91	96.30	96.28	81.40

Source: Authors (2024).

Table 6: Linear regression statistics

	STANDARD ERROR	COEF	P- VALUE	REGRESSÃO- F
C (mg. L^{-1})	0.000833	0.010384	0.000	1.00

Source: Authors (2024).

The material evaluated exhibits excellent sorption potential, surpassing, in some cases, values reported in the literature for materials traditionally used as sorbents. Similar values were observed by Santos [28] when investigating the adsorption capacity of sodium bentonite for cesium, further reinforcing the quality of the results obtained in this study. This demonstrates the feasibility of the geopolymer as an effective alternative for the removal of radioactive contaminants from aqueous radioactive waste.

4. CONCLUSIONS

Minerogical analyses confirmed the predominance of kaolinite and muscovite in the residue, aluminosilicate minerals whose layered structure favors reactivity during alkaline activation processes. Calcination at 800 °C promoted dehydroxylation and partial rearrangement of these phases, resulting in a more reactive precursor adequately conditioned for geopolymer synthesis.

The results of the thermal analyses enabled the identification of the temperature ranges associated with the main structural transformations, including dehydration, dehydroxylation, and the formation of intermediate phases, thereby validating the conditions adopted during the calcination step.

OPEN ACCESS

Alkaline activation of the residue allowed partial dissolution of the aluminosilicate species, leading to the consolidation of an amorphous matrix typical of geopolymers.

The final milling step increased the specific surface area and, consequently, the number of available sites for interaction with cationic species.

The results of the sorption experiments revealed that the resulting geopolymer exhibits high affinity for the Cs^+ ion, reaching a maximum adsorption capacity of 96.30 $mg \cdot g^{-1}$. This performance demonstrates the material's efficiency as a sorbent.

Therefore, it can be concluded that the integrated process comprising characterization, calcination, alkaline activation of the residue, and comminution of the geopolymer, was effective, enabling the production of a mining-residue-derived geopolymer with significant performance in cesium removal.

These results reinforce the potential of the material as a sustainable alternative for applications in containment systems and the treatment of radioactive effluents.

RECOGNITION

To CAPES and INCT Midas for sponsoring the scholarships and for encouraging the purchase of materials to carry out the tests.

FINANCING

To CAPES and INCT Midas for sponsoring the scholarships and for encouraging the purchase of materials to carry out the tests.

OPEN ACCESS

BY

CONFLICT OF INTEREST

We have no conflicts of interest to disclose. All authors declare no conflicts of interest.

DATA AVAILABILITY STATEMENT

The authors declare that the data supporting the results of this study are available in the article. Derived data supporting the conclusions of this study are available upon request from the corresponding author.

REFERENCES

[1]DA GAMA, E. M. et al. Study of Potential Use of Iron Mining Tailings Calcined in a Flash Furnace as Pozzolanic Material. **Current Innovations in Chemical and Materials Sciences.** Vol. 2, p. 178-196, 2023.

[2]BUCHWALD, A.; DOMBROWSKI, K.; WEIL, M.. **Development of Geopolymer Concrete Supported by System Analytical Tools**. Proceedings of the 2nd Int. Synposiun of Non-tradition Cement and Concrete, ed. by Bilek and Kersner, 25-35, 2005.

[3]DAVIDOVITS, J. **Environmentally driven geopolymer cement applications**. In: Proceedings of 2002 Geopolymer Conference. Melbourne. Australia. 2002.

[4]DA ROCHA, G. G. N. **Caracterização microestrutural do metacaulim de alta reatividade**. Dissertação de mestrado. Universidade Federal de Minas Gerais. Belo Horizonte, Minas Gerais, 2005.

[5]SARTI, M. E. V. et al. **Inertização de Resíduos Radioativos e Metais Pesados a partir da Imobilização Geopolimérica**. Trabalho de Iniciação Científica. Universidade Federal de Santa Catarina. Departamento de Engenharia Química e Alimentos. Graduação em Engenharia Química. 2023.

[6]PALMA, G. et al. **Optimization of Geopolymers for Sustainable Management of Mine Tailings: Impact on Mechanical, Microstructural, and Toxicological Properties**. Minerals, v. 14, n. 10, p. 997, 2024.

OPEN ACCESS

[7]PROVIS, J. L.; BERNAL, S. A. Geopolymers and related alkali-activated materials. **Annual review of materials research**, v. 44, n. 1, p. 299-327, 2014.

[8]PROVIS, J. L. Alkali-activated materials. **Cement and concrete research**, v. 114, p. 40-48, 2018.

[9]IAEA– INTERNATIONAL ATOMIC ENERGY AGENCY. **Selection of Technical Solutions for the Management of Radioactive Waste**. Vienna: IAEA. (IAEA-TECDOC-1817).2017.

[10]EL-NAGGAR, M. R., & AMIN, M. (2018). Impact of alkali cations on properties of metakaolin and metakaolin/slag geopolymers: Microstructures in relation to sorption of 134Cs radionuclide. **Journal of Hazardous Materials**, 344, 913–924. https://doi.org/10.1016/j.jhazmat.2017.11.049.

[11]ABNT – BRAZILIAN ASSOCIATION OF TECHNICAL STANDARDS. NBR NM 52, 2009. **Fine Aggregate – Determination of specific mass**. Rio de Janeiro, ABNT, 2009, p.3.

[12]ABNT – BRAZILIAN ASSOCIATION OF TECHNICAL STANDARDS. **Portland Cement – Determination of compressive strength of cylindrical specimens**, 2019. Brazilian Technical Standard (NBR) 7215:2019.

[13]SILVA, F.G.P; LAMEIRAS, F.S. **Desenvolvimento de argamassa geopolimérica com porosidade controlada.** Dissertação de Mestrado, Ciência e Tecnologia da Radiação, Minerais e Materiais, CDTN, Belo Horizonte, Minas Gerais, 2023.

[14]ENVIRONMENTAL PROTECTION AGENCY, EPA/530 SW-87-006-F: Technical Resource Document: Batch-type Procedures for estimating soil adsorption of chemical, 1992.

[15]FREIRE, C. B. **Estudo de Sorção de Césio e Estrôncio em Argilas Nacionais para sua utilização como barreira em Repositórios de Rejeitos Radioativos**. 2007. Dissertação (Mestrado em Ciência e Tecnologia das Radiações, Minerais e Materiais). Centro de Desenvolvimento da Tecnologia Nuclear (CDTN), Belo Horizonte, Minas Gerais, 2007.

[16]COLNAGO, L. R. L. et al. Preparation and characterization of geopolymers obtained from alkaline activated hollow brick waste. **Materials Research**, v. 27, n. Suppl 2, p. e20240203, 2024.

[17]SPARKS, D. L.; SINGH, B.; SIEBECKER, M. G. **Environmental soil chemistry**. Elsevier, 2022.

OPEN ACCESS

[18]KUMAR, S. G. K. M. et al. Geopolymer Chemistry and Composition: A Comprehensive Review of Synthesis, Reaction Mechanisms, and Material Properties. **Oriented with Sustainable Construction**. Materials, v. 18, n. 16, p. 3823, 2025.

[19]GRIDI-BENNADJI, F. et al. Structural transformations of muscovite at high temperature by X-ray and neutron diffraction. **Applied Clay Science**, v. 38, n. 3-4, p. 259-267, 2008.

[20]MANOSA, J. et al. Enhancing reactivity in muscovitic clays: Mechanical activation as a sustainable alternative to thermal activation for cement production. **Applied Clay Science**, v. 250, p. 107266, 2024.

[21]RRUFF. RRUFF Project – Mineral Database. Disponível em: https://rruff.info. Acesso em: 21 nov. 2024.

[22]BEN AMOR, A. et al. Clays-based geopolymers: a sustainable application as adsorbent of cytostatic drugs for water purification. **Applied Water Science**, v. 14, n. 11, p. 234, 2024.

[23]GENUA, F.; LANCELLOTTI, I.; LEONELLI, C. Geopolymer-based stabilization of heavy metals, the role of chemical agents in encapsulation and adsorption. **Polymers**, v. 17, n. 5, p. 670, 2025.

[24]DAVIDOVITS, J. **Geopolymer Chemistry and Applications.** 2. ed. Saint-Quentin, França: Institut Géopolymère, ISBN 978-2-9544531-1-8. 2008.

[25]LOEBENSTEIN, W. V. Adsorption, desorption, resorption**. Journal of Research of the National Bureau of Standards**. Section A, Physics and Chemistry, v. 67, n. 6, p. 615, 1963.

[26]GUGGENHEIM, S.; CHANG, Y.; KOSTER VAN GROOS, A. F. Muscovite dehydroxylation; high-temperature studies. **American Mineralogist**, v. 72, n. 5-6, p. 537-550, 1987.

[27]COPAJA, S. V.; FERRER, D. Study of the adsorption-desorption process of the metals: Cu, Mn, Pb and Zn IN VOLCANIC SOILS. **Journal of the Chilean Chemical Society**, v. 69, n. 2, p. 6140-6148, 2024.

[28] SANTOS, D. M. M. dos et al. Transporte de césio através de bentonita brasileira para ser utilizada como material de referência para barreiras de repositórios de superfície. Tese de doutorado. Centro de Desenvolvimento da Tecnologia Nuclear (CDTN/CNEN-MG), Belo Horizonte, MG (Brazil). 2021.

OPEN ACCESS

LICENSE

This article is licensed under a Creative Commons Attribution 4.0 International License, which permits use, sharing, adaptation, distribution and reproduction in any medium or format, as long as you give appropriate credit to the original author(s) and the source, provide a link to the Creative Commons license, and indicate if changes were made. The images or other third party material in this article are included in the article's Creative Commons license, unless indicated otherwise in the credit line to the material.
To view a copy of this license, visit http://creativecommons.org/licenses/by/4.0/.